Reprod. Nutr. Dev. 40 (2000) 127–148

Original article

The effects of dexamethasone on the differentiation and the fertilisation of the germinal primordium in the chick embryo

Danièle CUMINGE[a], Julian SMITH[b], Régis DUBOIS[a]*

[a] Institut d'Embryologie Cellulaire et Moléculaire, 49 bis avenue de la Belle Gabrielle, Collège de France et CNRS, 94736 Nogent-sur-Marne Cedex, France
[b] Centre de Biologie du Développement, Université Paul Sabatier, 31062 Toulouse, France

(Received 15 December 1999; accepted 24 February 2000)

Abstract — We showed that, in the chick embryo, the fertilisation of the attractive germinal epithelium by primary germ cells can be represented by a three-dimensional diagram in which the space and time co-ordinates are graduated in terms of the segmentation of the axial and paraxial mesoderm. We thus established that the differentiation of the coelomic epithelium into an attractive germinal epithelium and the fertilisation of the gonadal primordium both occur by mechanisms that are tightly linked to somitogenesis. In the continuous presence of a constant concentration of Dexamethasone, a marked inhibition of the rate of fertilisation of the gonadal primordium was observed. A mathematical analysis of the mode of action of the inhibitor revealed the progressive establishment of a competition between Dexamethasone and the molecule(s) responsible for the process of attraction. Given the chemical nature of the inhibitor, we propose that the endogenous factor that triggers the first step of the differentiation of the germinal primordium is a steroid-containing complex.

avian germ cells / chemotactism / differentiation / fertilisation / attractive field / steroid / dexamethasone

Résumé — Les effets de la dexaméthasone sur la différenciation et la fertilisation de l'ébauche gonadique chez l'embryon de poulet. La fertilisation du primordium gonadique par les cellules germinales primordiales (CGP) en transit dans la circulation embryonnaire est représentée par un diagramme à 3 dimensions dans lequel l'espace et le temps sont inscrits sur une graduation obtenue par la projection de la segmentation du mésoderme axial et paraxial. C'est la capture des CGP par chimiotactisme qui révèle l'existence et la localisation d'un champ attractif. Les gonocytes fixés dans l'ébauche gonadique sont les marqueurs de l'extension de celle-ci dans le sens céphalo-caudal. Il a ainsi été démontré que la différenciation de l'épithélium cœlomique en épithélium germinatif attractif (E.G) est étroitement couplée à la somitogenèse dans la région bornée par les somites 22 à 30. Ces observations posent le problème de savoir si la différenciation de l'E.G est progressivement déclenchée par les somites nouvellement formés, ou si elle est due à une propriété intrinsèque en

* Correspondence and reprints

corrélation avec le stade de développement de l'embryon. La discussion conclut en faveur de cette seconde hypothèse qui suggère le couplage de mécanismes génétiques homéotiques. En présence continue et à concentration constante de Dexaméthasone, une nette inhibition de la fertilisation de l'épithélium germinatif est observée. Le taux d'inhibition est proportionnel au logarithme de la concentration en corticoïde dans la gamme [10^{-9} M–10^{-5} M]. L'analyse mathématique du mode d'action de l'inhibiteur révèle l'établissement progressif d'une compétition entre la DEXA et le facteur chimique naturel qui déclenche le processus de capture des CGP dans les conditions normales du développement. Le mode d'action de la DEXA est discuté dans le cadre des acquisitions récentes sur la description des récepteurs des stéroïdes. La nature chimique de l'inhibiteur suggère que le facteur endogène qui active l'apparition des forces attractives du chimiotactisme est un complexe stéroïdien. Selon ces conceptions, c'est la mise en œuvre d'une machinerie moléculaire d'une extrême complexité, intégrant notamment un stéroïde et son récepteur cytosolique, qui déclenche la différenciation d'une région particulière de l'épithélium cœlomique en épithélium germinatif attractif.

cellules germinales des oiseaux / chimiotactisme / différenciation / fertilisation / champ attractif / stéroïde / dexaméthasone

1. INTRODUCTION

A previous study [7] has shown that the overall kinetics of fertilisation of the germinal epithelia (GE) of the chick embryo by primordial germ cells (PGC) conforms to the theoretical predictions of the logistic law (P.F. Verhulst, 1838; R. Pearl, 1924; see [21, 22]). In earlier work, the colonisation of the gonadal primordium was described in terms of a simple function of time. The present study completes previous preliminary investigations by considering an additional parameter, space {Sp}. Explicitly, we studied the variation of the numbers of gonocytes (Go) that become fixed at different levels of the gonadal primordium during development. The evolution of fertilisation of the GE by PGC transiting in the embryonic circulation is represented in a three-dimensional grill in which the number of gonocytes captured (N) is a point function of the form: $N = f[(t), \{Sp\}]$.

In the second part of this study, we developed the analysis and interpreted the experimental results obtained using Dexamethasone (DEXA) in this system. For reasons that are presented in detail in our earlier work [8], our observations are described within the framework of the chemotactic theory of migration of chick PGC: the notions of "attractive forces" and "attractive field" are extensively used in the text.

2. MATERIALS AND METHODS

The development of the chick embryo is classically described in terms of a "biological" progression in which morphological aspects play a key role. This option for a time axis (t) graduated by a succession of somitic stages (s) is explained by the fact that fertilised eggs are laid at different stages and attain given degrees of development after periods of incubation that can be very variable. In the present work, the somitic stage was used as a co-ordinate either of time (t) according to Hamburger and Hamilton [14] or of space {Sp} along the anteroposterior axis. We designate the time co-ordinate by (s) and the space co-ordinate by {s}.

Observations under normal conditions were made on Hubbard chick embryos cultured on a gelose-containing medium [32]. Blastoderms, explanted at the 20-somite stage, were cultured at random for different times up to the 28-somite stage. Beyond this point the fertilisation process is disturbed by the proliferation of the gonocytes installed in the germinal epithelia. At the end of its imparted culture period, each

blastoderm was fixed in toto in Halmi solution. The gonadic regions were dissected at the level of the 19th pair of somites and reoriented as accurately as possible during their subsequent inclusion in paraffin, with the aim of facilitating the identification of homologous pairs of somites on cross sections. Whenever the homologous somites were not rigorously parallel to the plane of the section, the observer made corrections, which have a potential resolving power equal to the thickness of a section, that is 6.6 μm. Gonocyte counts in the GE were carried out on sections stained with glychaemalun-eosin.

The spatial co-ordinate {Sp} of the gonadal primordium was defined as follows: the segmentation of the paraxial mesoderm into somites is projected on the coelomic epithelium. One thus obtains an imaginary, anatomically continuous subdivision of the gonadal primordium into a series of {s} and {i-s} regions that follow each other in phase with the sequence of somitic and intersomitic spaces of the segmented paraxial mesoderm. This virtual regionalisation of the GE allowed an interesting sectorial analysis to be made of the evolution of the colonisation processes, as will be apparent later (see Results). Finally, the numbers of histological sections of the total gonadal region, as well as of the {s} and {i-s} regions, were noted, in order to determine the density of gonocytes ($Go \cdot mm^{-1}$) in these different compartments.

Dexamethasone (9α – Fluoro – 16α – methyl – 11β – 17α, 21 – trihydroxy – 1,4 – pregnadiene – 3,20 – dione – 21 – acetate; Sigma) was dissolved in Tyrode solution, at concentrations from 10^{-9} M to 10^{-5} M. When the blastoderms reached the 20-somite stage (20s) in ovo, they were immersed for several minutes at 38 °C in a glucocorticoid solution at a concentration of C_X (i.e. 10^{-x} M). They were then transferred to a gelose-based medium (also containing DEXA at C_X), according to the technique of Wolff and Simon [33], from which randomly chosen blastoderms were removed and fixed in Halmi at a time (t) within the interval [(24s) to (28s)]. For a concentration C = 10^{-5} M, the interval extended from stage (26s) to stage (28s). Histological preparations were prepared and analysed as described for the control embryos.

3. RESULTS

3.1. Properties of the control population: three-dimensional analysis of the fertilisation of the germinal epithelium

The results were obtained from a series of 191 blastoderms selected from a population of 271 explants. Embryos exhibiting abnormal development or cardiovascular defects (haemorrhage, venous stasis or ischaemic zones) were excluded from the statistics (it has been shown that haemodynamic plays an important role as an external cause of chemotactism in the fertilisation of the gonadal primordium [8, 16].

3.1.1. Colonisation of the GE as a function of time(s)

The results are displayed in Table I and are expressed graphically as a function of stage (time) by curve 1 in Figure 1 (●). For comparison, the results (o) obtained in a previous study [7] are included. There was an excellent agreement between the two series of measurements within the limits of experimental error. The value of the asymmetry index, which depends both on attractive forces and haemodynamic parameters [8], was thus confirmed (Tab. I, column 2).

3.1.2. Properties of the imaginary {s} and {i-s} regions of the gonadal primordium at different stages of development

In order to compare the measurements more easily, the results are presented in

Table I. Properties of the control sample.

Stage (time)	cases (n)	N_C ^{X} (± SEM)	Asymmetry (G%) *			Length (mm) ❑ Density (Go.mm^{-1})		
			T_1	{s}	{i-s}	T_2	{s}	{i-s}
Columns		1	2	3	4	5	6	7
22s	16	2.44 (3)	◊					
23s	38	9.5 (1)	52 (3.5)	51 (4)	55 (6)	0.450 21	0.324 20	0.126 24
24s	25	22.2 ⊗ (2)	62 (3)	65 (3)	58 (7)	0.584 38	0.438 40 ⊗	0.145 34 ⊗
25s	30	37 ⊗ (4)	65 (1.2)	66 (3)	59 (4)	0.713 52	0.520 50 ⊗	0.193 55 ⊗
26s	40	78.5▲ (5.6) ⊗	62 (2)	61 (2)	64 (3)	0.780 100	0.554 100▲ ⊗	0.226 105▲ ⊗
27s	27	105▲ (8) ⊗	65 (1.6)	66 (3)	65 (2)	0.890 115	0.658 118▲ ⊗	0.232 109▲ ⊗
28s	15	144▲ (13) ⊗	59 (3)	58 (3)	60 (3)	1.080 133	0.800 136▲ ⊗	0.280 122▲ ⊗
total : 191		C_1(•) ▲	61%	61%	60%	Relative Length	73%	27%

N_C^X : Arithmetic mean of the number of gonocytes captured per embryo at the stage considered. Kinetics represented by curve C_1. (Fig.1).

G%* : Asymmetry of distribution of PGC in favour of the left side.

❑ : Space occupied in the gonadal region ; regions {s} and {i-s}.

Go.mm^{-1} : Gonocyte density in the entire attractive GE (T_2), regions {s} and {i-s}.

⊗ , ▲ : Values for the determination of the law of inhibition : see tables III and V.

◊ : Results not statistically significant.

T_1 , T_2 : The entire germinal primordium.

Table I, columns 3–7. The asymmetrical distribution of PGC in the {s} and {i-s} regions, with a bias towards the left side, was statistically similar to that observed in the whole primordium (column 2). There were no significant differences with regard to this characteristic between regions that were exposed to the {s} somites and {i-s} regions. The same was true of gonocyte density (Go·mm^{-1}). It should be noted that the entire {s} region occupies approximately 73% of the length of the gonadal region, regardless of the stage at which the measurement was made.

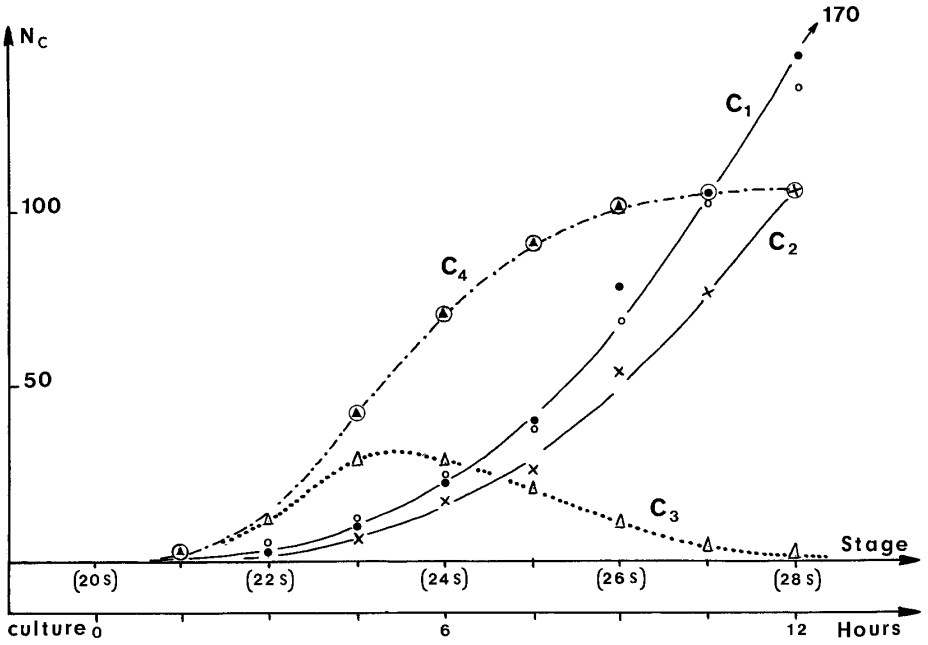

Figure 1. Kinetics of the fertilisation of the germinal epithelium. C_1: variation of the numbers of gonocytes (N_C) captured in the gonadal region as a function of stage (s) or time (t); see Table I, column 1. The (○) indicate the values obtained in earlier experiments [7] in which the number of PGC colonising the GE was shown to tend towards a maximal value of 170 (see text Part II and Tab. VI bis). C_2: variation of the numbers of gonocytes installed in all the imaginary {s} regions *as a function of time* (Tab. II, last column). C_3: Numbers of gonocytes installed in each {s} region at the end of the observation period (stage 28s). C_4: variation of the numbers of gonocytes captured in the {s} regions *as a function of space {Sp}*. Integral curve of C_3; cf. kinetic represented in C_2
N.B.: The correspondence between time in culture and developmental stage (expressed in "somite-units") is approximate. Variation of the numbers of gonocytes (N_C) as a function of time (t) *and* space {Sp}: see Figure 2.

3.1.3. Capture of the PGC in the imaginary {s} regions as a function of space [{Sp} = {s}] and time [(t) = (s)]

The results are summarised in Table II and represented graphically in Figure 1. The kinetics of colonisation of the zone corresponding to the sum of all the {s} regions (Tab. II, last column) are presented graphically by curve 2 in Figure 1. Each point (X) represents the sum of the numbers in columns {20s} to {28s} for each stage in the interval [(20s) to (28s)]. Curve 2, which does not take into account local events peculiar to each {s} region, is merely the result of the application to curve 1 of the coefficient 0.73 corresponding to the part of the gonadal primordium occupied by the {s} regions over time.

Our data also took into account the role played by the hypothetical regionalisation of the gonadal primordium by considering the kinetics of colonisation at the end of the period of observation as a function of space. Thus at stage 28s, the total number (Δ) of gonocytes installed in each {s} region was evaluated during the period [(20s) to (28s)] (curve 3); the kinetic represented graphically

Table II. Number of gonocytes installed in the imaginary {s} regions of the germinal primordium at different stages of development.

(S) ↓	{20}	{21}	{22}	{23}	{24}	{25}	{26}	{27}	{28}	Regions ← {s}	
22s	0.33 (0.16)	0.53 (0.24)	0.53 (0.21)	0 [						1.4	/
23s	0.37 (0.15)	1.5 (0.3)	1.9 (0.3)	2.9 (0.5)	0 [					6.7	/
24s	0.29 (0.21)	0.46 (0.2)	4.25 (0.6)	8.04 (1.0)	3.96 (0.5)	0 [				17	⊗
25s	0.27 (0.15)	2.6 (0.7)	5.83 (0.8)	9.2 (1.2)	5.66 (0.7)	2.53 (0.4)	0 [			26.1	⊗
26s	0.30 (0.11)	2.8 (0.6)	11.8 (1.3)	16.8 (1.4)	12.6 (1.2)	6.9 (0.9)	3.5 (0.5)	0 [		54.7	▲ ⊗
27s	0	1.55 (0.4)	12.5 (2.0)	23.5 (2.2)	20 (1.5)	11 (1.3)	6.3 (0.8)	1.8 (0.4)	0 [	76.6	▲ ⊗
28s	0 → $C_3\Delta$	2 (0.7)	11.3 (1.7)	28.8 ♦ (4.0)	28.1 (2.4)	20.3 (2.7)	10.3 (1.8)	4.0 (1.3)	1.0 (0.4) [	105.8	▲ ⊗
ΣNc (28s)	C_4 ▲ →	2	13.3	42.1	70.2	90.5	100.8	104.8	105.8	C_2X	✻
(27s)→(28s)	/	/	5	8	9	4	2	1	See text		

C_2^X , $C_3\Delta$, C_4▲ : See graphs in figure 1.

♦ : See Tables IV & VI and figure 2.

✻ : In the last column, the ▲ denotes the extreme values of the kinetic processes taken into account, in the controls, to determine the law of inhibition within the interval [(26s)-(28s)] ;

⊗ idem for the entire period over which the measurements were made [(24s)-(28s)].
See part II, law of inhibition in the presence of DEXA (Table V).

The symbols [indicate the anterior limit of the unsegmented paraxial mesoderm.

in Figure 1, curve 4 was obtained from the evolution of the sum of the numbers in line ΣN_C of Table II.

By comparison with graph 2 (or 1), graph 4 provides interesting information about spatio-temporal events. Thus, whereas curve 2 shows that during the time required for the formation of the 28th somite, the total number of gonocytes captured by the entire {s} region increased by 29 units, curve 4 provides more detailed information about this phenomenon: of the 29 new gonocytes captured, 13 were installed in regions {23s} and {24s}, 13 in regions {25s} and {26s} and only 3 in regions {27s} and {28s}, (see Tab. II, last line). Furthermore, the kinetics with respect to space are represented by an S-shaped curve whose asymptotic values can easily be extrapolated from the measured points. This was put to advantageous use in interpreting the experimental results (see Tabs. IV and V). In conclusion, whereas each measurement in Table II was made during the course of development at a given time and in a given sector of the gonadal rudiment, by means of this method of analysis, the evolution of the process of fertilisation of the gonadal rudiment can be described as a function of space and time (Fig. 2).

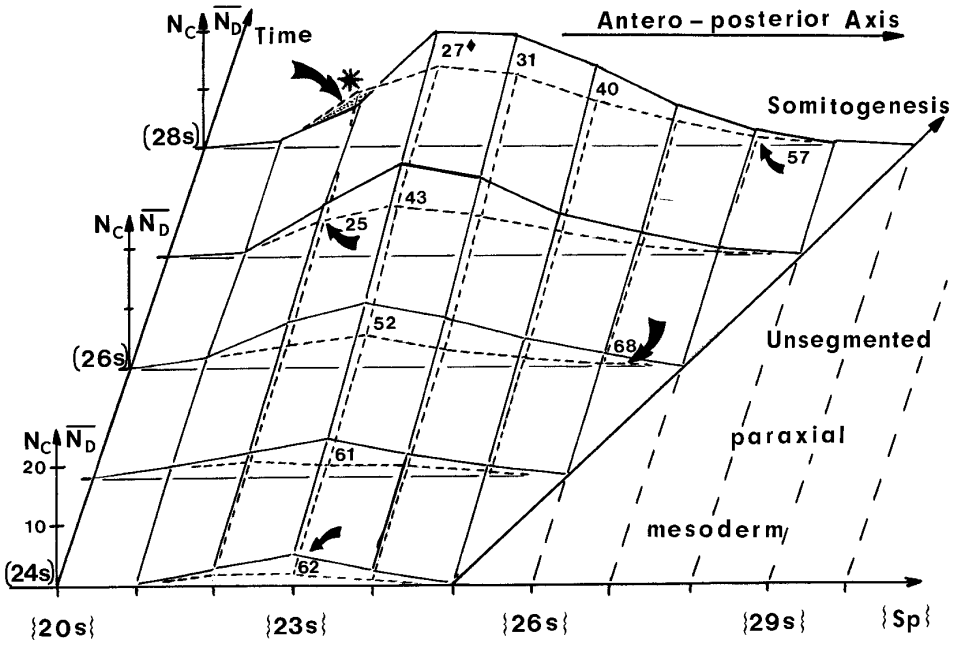

Figure 2. Propagation of the wave of fertilisation with respect to space {sp} and time in the {s} regions of the germinal primordium. *Solid lines*: Normal developmental conditions (Tab. II). There is a strict spatio-temporal correspondence between the surge of the attractive field and progressive somitogenesis. *Dashed lines*: The same process in the presence of DEXA at a mean concentration of 4.6×10^{-8} M (see part II: variations of $\overline{N_D}$, Tab. IV). The two diagrams were synchronous but display numerous disparities (e.g. where indicated by bold arrows): variations in the level of inhibition in space and time (see Tab. VI, Sect. 1). ✻: "paradoxical" situation in which the number of gonocytes captured in the presence of the inhibitor is greater than in the controls (see Tabs. VI and VI bis, and Fig. 5).

3.1.4. Spatio-temporal representation of the wave of fertilisation; commentary on Figure 2

The graphical representation (solid lines) reflects the propagation of a wave of fertilisation which synchronously accompanies the surge of attraction resulting from the differentiation of the gonadal primordium (first step in sexual organogenesis). This wave has a remarkable property: irrespective of the stage, it (like the attractive field that its existence reflects) never crosses the frontier that is the posterior limit of the segmented paraxial mesoderm. Beyond this frontier, the coelomic epithelium which borders the non-segmented paraxial mesoderm does not capture a single PGC, despite the presence of these cells in the embryonic circulation that irrigates this region. This epithelium should thus be considered as a presumptive GE in which the mechanisms of differentiation into an attractive epithelium are not activated. The differentiation of the coelomic epithelium into an attractive GE follows an approximately cranio-caudal progression in the [{22s}→{30s}] region in tight spatio-temporal correlation with somitogenesis. This virtual segmentation of the gonadal epithelium reveals that, in reality, the differentiation of an anatomically uniform organ is sequentially directed by mechanisms that depend on the antero-posterior plan of organisation. Detailed analysis revealed that the wave of fertilisation displays a peak at the level of regions {23s}

and {24s}. This peak corresponds to the expression of maximum intensity of the attractive forces in this zone of the gonadal primordium. The latter remained attractive at all levels within the time interval [(22s) to (28s)].

For convenience and brevity, we only considered the results obtained in the {s} regions. The data relative to the {i-s} region can be easily calculated from the data in Tables I and II. The representation provided in Figure 2 can be extrapolated to the entire gonadal region.

3.2. The effects of dexamethasone on the fertilisation of the germinal epithelium

In a previous study [16], Jakubowicz showed that low concentrations (in the

Table III. Properties of the sample cultivated in the presence of Dexamethasone (289 cases; overall measurements).

DEXA Concentration	Stage (time)	Cases (n)	N_D (± SEM)	Asymmetries G% T_1	Asymmetries G% {s}	Asymmetries G% {i-s}	Density (Go. mm^{-1}) T_2	Density (Go. mm^{-1}) {s}	Density (Go. mm^{-1}) {i-s}
Columns →			1	2	3	4	5	6	7
10^{-9} M	24s	8	16.6 (3)	67	67	65	28	28	29
	25s	15	25.2 (3)	67	67	62	35	36	34
	26s	27	42 (4) ▲	65	66	61	52	54 ▲	46 ▲
	27s	27	86.5 (7) ▲	65	65	66	89	90 ▲	89 ▲
	28s	8	118 (13) ▲	57	57	56	108	112 ▲	94 ▲
	Σn	85	$\overline{57.7}$ ⊗					$\overline{64}$ ⊗	$\overline{58.4}$ ⊗
10^{-7} M	24s	10	13.7 (6)	59	56	64	24	21	32
	25s	24	22.8 (2)	53	52	54	32	30	37
	26s	28	35.7 (6) ▲	62	63	61	41	93 ▲	93 ▲
	27s	25	53 (5) ▲	62	62	58	53	93 ▲	93 ▲
	28s	10	99 (14) ▲	60	58	63	91	89 ▲	93 ▲
	Σn	97	$\overline{44.8}$ ⊗					$\overline{46.4}$ ⊗	$\overline{52.4}$ ⊗
10^{-6} M	24s	34	13.3 (2)	69	68	69	22	23	20
	25s	14	21.6 (4)	68	71	59	30	29	31
	26s	14	31.2 (4) ▲	63	63	67	35	35 ▲	35 ▲
	27s	11	50 (6) ▲	62	64	58	47	45 ▲	51 ▲
	28s	4	86 (9) ▲	62	63	60	78	78 ▲	78 ▲
	Σn	77	$\overline{40.4}$ ⊗					$\overline{42}$ ⊗	$\overline{43}$ ⊗
10^{-5} M	26s	5	21.2 (4) ▲	47	51	44	31	32 ▲	27 ▲
	27s	10	31 (6) ▲	62	61	65	37	38 ▲	37 ▲
	28s	15	46 (5) ▲	53	54	52	43	44 ▲	42 ▲
	Σn	30	$\overline{32.7}$ ▲					$\overline{38}$ ▲	$\overline{35.3}$ ▲

N.B. Illustration of the method of calculating the law of inhibition (Table V, Figure 3a) : duration of the experiment [(26s)-(28s)] ; DEXA concentration = 10^{-7} M.

$\overline{N_C}$ = (78.5 + 105 + 144) / 3 = $\overline{109.16}$ (Table I, column 1, ▲)

$\overline{N_D}$ = (35.7 + 53 + 99) / 3 = $\overline{62.56}$ (Table III, idem)

Percentage inhibition = [(109.16 - 62.56) / 109.16]. 100 = 42.7%,*, see Table V.

Table IV. Number of gonocytes installed in the imaginary {s} regions in the presence of DEXA.

DEXA concn.	Stage (t)	Number N_D of gonocytes captured in {s} regions									Cumulated numbers	
		{20s}	{21s}	{22s}	{23s}	{24s}	{25s}	{26s}	{27s}	{28s}		
	24s	1	2	3.6	3.5	2.7	0				12.8	
10^{-9} M	25s	1.9	3	4.2	3.8	3.7	1.5	0			18.1	
(n=85)	26s	0.6	2.6	5.4	9.7	5.8	3.8	1.9	0		29.8	▲
	27s	0.3	2.2	12.5	18	15	9	4.3	0.4	0	61.7	▲
	28s	0.7	2	18	24 ◆	22	14	7	2	0.1	89.8	▲
10^{-9} M											42.4	⊗
	24s	0	1.2	2.6	2.8	1	0				7.6	
10^{-7} M	25s	1.5	2.7	3.2	3.5	2.5	1.3	0			14.7	
(n=97)	26s	0.4	1.8	7	8	4.5	3	1	0		25.7	▲
	27s	0.2	2.4	7.2	11.2	9.2	5.4	3.2	1	0	39.8	▲
	28s	0	1.1	8.1	19.2◆	17.7	15.5	8.2	2.2	1	73	▲
10^{-7} M											32.16	⊗
	24s	0.5	1.3	3.1	2.9	1	0				8.8	
10^{-6} M	25s	0.2	2.6	5	3.3	2.5	0.9	0			14.5	
(n=77)	26s	0.7	2.8	6	6.4	3.8	0.3	0.5	0		20.5	▲
	27s	0	2	8.3	11	7	3.8	1.5	0.9	0	34.5	▲
	28s	0	2.2	12.5	19.7◆	18.2	7	4	1	0	64.6	▲
10^{-6} M											28.6	⊗
	26s	0.8	2.2	5	4.8	3	2.3	1	0		19.1	▲
10^{-5} M	27s	0.1	2.7	3.4	6.9	5	2.6	0.8	0.3	0	21.8	▲
(n=30)	28s	0.2	1.1	8	10.6	8	3.5	2.2	0.6	0.1	34.3	▲
10^{-5} M											25.1	▲

From this table, one can determine :
1./ The law of inhibition from the kinetic data (Tables II and IV).
example : DEXA concn = 10^{-6} M ; interval [(24s)-(28s)] ; results ⊗
Controls : 56.04 ; Experimental embryos : 28.6.
% inhibition : [(56.04 - 28.6) / 56.04]. 100 = 49% # (see Table V, 2)
2./ The properties of the attractive field in the presence of DEXA (Fig.2). A different algorithm is used to calculate the degree of inhibition in each {s} region at each (s) stage. An example is provided in the text, Part II, paragraph 3. See table VI and figure 2.

10^{-7} M range) of Dexamethasone (a non-metabolisable analogue of corticosterone) strongly inhibit the colonisation of the gonadal primordium in the chick. The author noted that the extent of inhibition increases as a function of the concentration of DEXA, although she was not able, from the measurement carried out, to define the mathematical form of the relationship.

Here we extended these preliminary observations by applying techniques based on the methodology described in materials and methods. Of a total of 380 blastoderms cultured under these conditions, 91 abnormal embryos (see Part I) were discarded. Using a sufficiently sound statistical base (289 cases divided into four experimental groups), we were able to mathematically formulate the inhibition process.

3.2.1. Properties of the experimental samples as a function of stage

The quantitative data are presented in Tables III and IV, which are homologues of Tables I and II respectively. A comparison of

Tables I and III (columns 1) revealed an unquestionable inhibitory effect of DEXA: the differences between control and experimental embryos were significant to 5% at the lowest concentration of the inhibitor 10^{-9} M). At concentrations $\geq 10^{-7}$ M, the probabilities that the differences observed at stages (24s) to (28s) were due to chance fluctuations were $\leq 10^{-2}$ and reached values of $\leq 10^{-6}$. The left-hand bias of the asymmetry of distribution of the gonocytes was not significantly modified (columns 2, 3 and 4). The external factors that influenced the fertilisation of left and right gonadal primordia were not disturbed in the presence of DEXA: consequently, the glucocorticoid must have acted on the motility of the PGC and/or the attractive forces exerted by the germinal epithelium. This was in agreement with the results obtained by Jakubowicz [16]. Finally, it should be noted that the values of gonocyte density ($Go \cdot mm^{-1}$) were invariably lower in experimental embryos than in the control without there ever being significant differences between imaginary regions {s} and {i-s} in the primordia (columns 5, 6 and 7).

3.2.2. Mathematical formulation of the law of inhibition (Tab. V, Fig. 3)

The form of the relationship between the degree of inhibition (by comparison with the controls) and the concentration of the inhibitor is of particular interest, for it can often lead to plausible hypotheses that explain the results obtained. An example is the inhibition of the colonisation of the gonadal epithelium by Concanavalin A, a binary "all or nothing" effect that designates the PGC as the targets of lectin (see discussion). In order to determine with certainty the nature of the law governing the inhibition by DEXA, we took the following variables into account:

(a) (N_C) and (N_D) in Tables I and III, columns 1;

(b) ($Go.mm^{-1}$, {s}) and ($Go.mm^{-1}$, {i-s}), Tables I and III, columns 6 and 7;

(c) the limiting values to which the kinetics of fertilisation of regions {s} tend as a function of space (Tabs. II and IV, last columns).

N.B., the parameters (N) and ($Go \cdot mm^{-1}$) are doubtless tightly correlated, but their variations were not rigorously identical. Both were the objects of natural individual fluctuations, as well as the techniques used for enumerating the gonocytes. In addition, ($Go \cdot mm^{-1}$) was subject to a random influence related to the individual variability of the extension of regions {s} and {i-s} and to the analysis of the histological sections.

Data processing

It is clear that the variation of (N_C) at different stages of development are subject to natural statistical fluctuations, often of considerable amplitude [7] and the same applies to the values of (N_D) under experimental conditions. One can even out these discrepancies from the means (N_C) and (N_D) by increasing the number of measurements and by using the maximum of information at our disposal. This aim was achieved by performing calculations on the arithmetic mean of measurements carried out at the different stages of the experimental interval [(26s) to (28s)], during which four concentrations of DEXA (ranging from 10^{-5} M to 10^{-9} M) were tested. In Tables I to IV these measurements are distinguished by the sign (▲); the corresponding graph is presented in Figure 3a. In order to facilitate the reading and the interpretation of the data, an example of the development of the calculations is provided in the lower part of Table III.

In addition, as will be pointed out later, it is informative to analyse the ongoing processes over a period that is longer than the previous interval. The law of inhibition was determined within the interval [(24s) to (28s)], for which the concentrations of DEXA were $\in$ [10^{-6} M, 10^{-7} M and 10^{-9} M]. The corresponding measurements are identified by the sign ⊗. Table V contains the results of

Table V. Mathematical expression of the law of inhibition (see Fig. 3; global data from Tabs. I to IV).

Data included in the calculation :		DEXA concentration 10^{-9} M	10^{-7} M	10^{-6} M	10^{-5}M
1) Tables I and III					
a/ variables : N_C & N_D	▲	24.7	42.7 ✶	48.9	70
	⊗	25.6	42	47.7	/
b/ variable : Go. mm^{-1} {s}	▲	27.7	48.9	55.4	67.8
	⊗	27.9 ●	47.7	52.7	/
c/ variable : Go. mm^{-1} {i-s}	▲	31.8	42.6	51.2	68.5
	⊗	31.3	38.3	49.4	/
2) Tables II and IV					
Variable : Kinetics	▲	23.5	41.6	49.5	68.3
	⊗	24.3	42.6	49 #	/
3) Means %					
Fig. 3a	▲	27	43.9	51.2	68.6
Fig. 3b	⊗	27.2	42.6	49.7	/

Example of calculation : $\overline{(\text{Go. mm}^{-1}, \{s\})_C} = \overline{88.8}$; % = 27.9 ●

$\overline{(\text{Go. mm}^{-1}, \{s\})_D} = \overline{64}$

42.7% ✶ and 49% # : for the determination of these values, see notes to the Tables III and IV respectively.

the calculations, and the corresponding curves are presented in Figures 3a and 3b. A consideration of the equations for the corresponding regression lines shows that the law of inhibition is expressed in a virtually identical manner, within the limits of statistical fluctuations: in order to interpret the results obtained during the experimental period [(24s) to (28s)], it is thus legitimate to exploit the law of inhibition (Fig. 2, diagram in dashed lines).

3.2.3. Properties of the wave of fertilisation in the continual presence of Dexamethasone (Fig. 2)

In order to facilitate the comparison of measurements made on control and experimental embryos, the curve representing the development of the attractive field under experimental conditions has been included in Figure 2. The spatio-temporal extension of the two waves of fertilisation, closely linked to somitogenesis, is described by the diagrams in solid and dashed lines. A comparative analysis of the data in Tables IV and II enabled the effects of DEXA to be determined. This analysis was performed in accordance with the following methodological conventions:

– the entire experimental period was studied, which implies that, within interval [(24s) to (28s)], only concentrations 10^{-6} M , 10^{-7} M and 10^{-9} M (mean = 4.6×10^{-8} M) were taken into consideration;

– for the sake of conciseness in the treatment and the graphical presentation of the results, and to even out statistical fluctuations, the calculations were made on the arithmetic mean of the three values of N_D (Tab. IV) obtained in each {s} region at each (s) stage for all three inhibitor

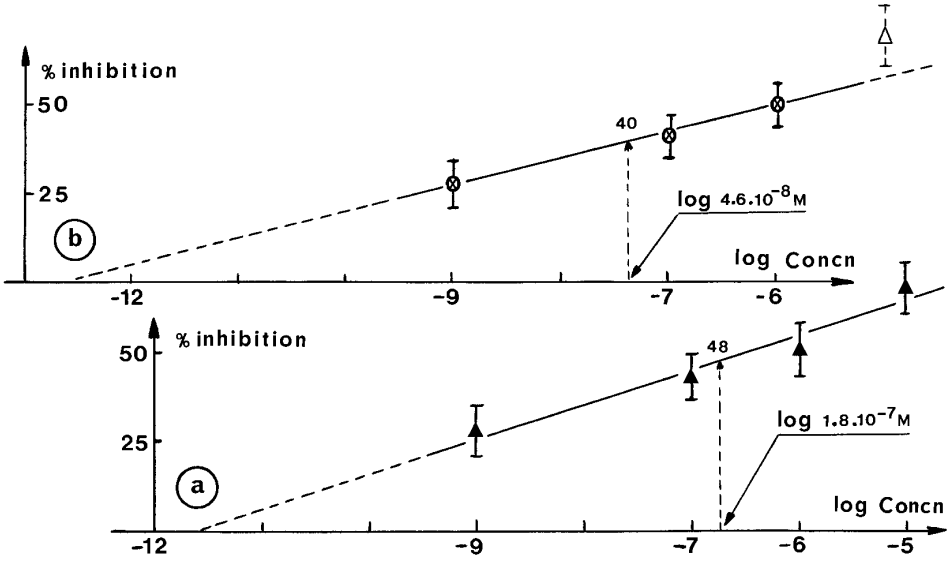

Figure 3. Law of inhibition of fertilisation in the presence of dexamethasone (Tab. V). (**a**) Equation of linear regression for the period [(26s) to (28s)]. Concentrations of DEXA: C ∈ (10^{-9} M ... 10^{-5} M). % inhibition = 9.8 log (C/Co) with Co = 2.4×10^{-12} M. (**b**) Equation of linear regression for the period [(24s) to (28s)]. Concentrations of DEXA: C ∈ (10^{-9} M; 10^{-7} M; 10^{-6} M). % inhibition = 7.5 log (C/Co) with Co = 2×10^{-13} M. The confidence limits are given for a confidence level of 95%. In each case, the mean concentration corresponding to the arithmetic mean of the logarithms on the abscissa, and the corresponding mean degree of inhibition are indicated.
N.B.: For a given concentration of DEXA, the degree of inhibition varies in space and time (see Tab. VI and Figs. 2 and 4): the law of inhibition is the resultant of complex events and should be interpreted at the level of the global evolution of the attractive germinal primordium (see text).

concentrations. Thus, at stage (28s), for example, the "mean" level of inhibition in the {23s} region was calculated using the following algorithm (Tab. IV, second interpretation of the data):

$\overline{N_D}$ = (24 + 19.2 + 19.7)/3 = 20.9 gonocytes captured in the presence of DEXA (Tab. IV, ◆). The control value being 28.8 (Tab. II, ◆), the coefficient of inhibition was therefore (28.8–20.9)/28.8 = 0.27 ◆; this corresponds to the "theoretical mean" concentration of 4.6×10^{-8} M DEXA (Fig. 3b and Tab. VI, Sect. 1). The mathematical expression of the law of inhibition enables the data to be treated in this way, since the degree of inhibition was proportional to the log of the concentration of DEXA. The figures provided in Table VI, section 1, are the result of the application of this calculation to each of the {s} regions in the space interval [{22s}→{28s}] for each stage within the time period [(24s) to (28s)]; a graphical representation is provided in Figure 2 (dashed lines). In Figure 2, one can note a strict synchronism associated with the coincidence of the spatial extensions of the phenomena studied. The inhibitory effect is tightly coupled to the propagation of the attractive field (already described in Part I). The two diagrams are not, however, ideally similar since there are obvious departures from the proportionality that should, according to the law of inhibition, govern the intensity of PGC flux.

Clearly, this law only holds for the overall event (Fig. 3 and its explanation), as is illustrated by the examples of values of the level of inhibition that are superimposed on the diagrams. Despite the presence of DEXA throughout the experimental period (at a constant concentration, as we shall see later), the degree of inhibition was not constant and this variability caused numerous anomalies of the congruence of the two representations (some of the most flagrant are highlighted by the bold arrows on the diagrams).

In particular, in the arbitrary example chosen, it can be noted that the degree of inhibition characteristic of the {23s} region decreased regularly with time (Tab. VI). Likewise, a horizontal reading of the diagrams, as a function of space {Sp}, shows that the most anterior regions in the space [{22s}→{24s}] showed a level of inhibition that was considerably lower than measured in posterior regions, close to the front of the spreading attractive field. Thus, at the end of the experiment, as one explored the attractive field in the direction of its propagation, the inhibitory effect increased. This observation suggests that, in the continual presence of the inhibitor, the intensity of the fertilisation processes in the most anterior regions (both in time and space) increased regularly as a result of the recovery of the attractive forces and/or the migratory properties of the PGC transiting in the circulation.

3.2.4. Analysis of the mode of action of Dexamethasone (Tabs. VI and VI bis, Figs. 4 and 5)

There is thus evidence for the existence of a phenomenon that antagonises the inhibitory effect and results in the progressive recovery of the intensity of the fertilisation process.

Since they concern the experimental period [(24s) to (28s)], the calculations took into account the methodological conventions detailed in the previous section. They were first made using the data in Tables II and IV and the results appear in Table VI, Section 1; the degree of inhibition for each pair ((s) – {s}) is given by $[(N_C - \overline{N_D}) / N_C] \times 100$.

Commentary and explanation of Table VI

Considered as a whole, the data in this Table (Sect. 1), derived from the diagram in solid lines (Fig. 2), allowed a graphical representation of the spatio-temporal properties of the wave of fertilisation in the presence of the inhibitor (Fig. 2, dashed lines). In addition, an examination of the measurements symbolised by points (■) revealed that the degree of inhibition remained constant in the {s} regions situated at the leading edge of the wave of fertilisation (and thus of the attractive field). Each of the five *successive measurements* enabled the degree of inhibition to be determined in a particular $\{n_s\}$ region at the time that the (n_s) somite formed from the unsegmented paraxial mesoderm. The local extent of inhibition measured under these conditions was approximately 60% for a DEXA concentration of 4.6×10^{-8} M (Fig. 4, line D_1). This was in agreement with the fact that the inhibitor was continually present, at a constant concentration, during the experimental period.

On the contrary, if the degree of inhibition was measured *simultaneously* in the different {s} regions, the result was completely different and in contradiction with the above mentioned observation. Such was the case for the data symbolised by points (●) in Table VI, Section 1, last line, which were obtained at the end of the experiment (stage 28s). As one scans the gonadal primordium in a caudo-cranial direction from the position of the last formed somite, the degree of inhibition diminished progressively. Under these conditions (Fig. 4, line D_2), the mean value for the entire gonadal primordium was around 40% at a DEXA concentration of 4.6×10^{-8} M also the explanation of Fig. 3). When the

Table VI. Degree of inhibition in the different imaginary {s} regions as a function of the stage, at a mean DEXA concentration of 4.6×10^{-8} M.

1/ Overall data N_C and $\overline{N_D}$ (Fig.2) : apparent values.

Space / Time	{22s}	♦ {23s}	{24s}	{25s}	{26s}	{27s}	{28s}	Figure 4 ↓
(24s)	27	62	60 ■					
(25s)	29	61	49	51 ■				
(26s)	48 (50)	52 (57)	63 (66)	66 (66)	68 ■ (69)			
(27s)	25 (37)	43 (50)	48 (55)	45 (53)	52 (61)	57 ■ (64)		
♦(28s)	✳ (✳)	♦ 27 (36)	31 (41)	40 (51)	38 (48)	57 (64)	63 (70)	D_2 / D_1

2/ Determination of inhibition on the basis of the increases ΔN_C and $\overline{\Delta N_D}$ (Fig. 5 and Table VI bis) ; real values

Interval								
[(24s)-(26s)]	60	43	64	67	66	/	/	/
[(26s)-(28s)]	✳ (✳)	✳ (7)	6 (21)	27 (43)	22 (38)	57 (64)	63 (70)	/
[(27s)-(28s)]	✳ (✳)	✳ (✳)	✳ (8)	34 (43)	15 (28)	56 (64)	64 (70)	Figure 5 /

N.B. Values in brackets apply to a mean concentration of $1.8.10^{-7}$ M Dexa
■ and ●: lines D_1 and D_2, Figure 4.
♦ For an example of calculation, see text (Part II, paragraph 3)
✳ Number of gonocytes captured in the presence of DEXA is greater than in controls (see Table VI bis and figure 5).

calculations were made for the experimental period [(26s) to (28s)], the results were virtually identical (numbers in brackets). The average value for the gonadal primordium was then approximately 50% when the DEXA concentration was 1.8×10^{-7} M (Fig. 3a).

Since the different values of the degree of inhibition at different levels of the primordium were measured *simultaneously*, the observed effect could not be due to the migratory characteristics of the PGC, randomly circulating in the blood flow, which should be considered as constituting an essentially homogeneous population.

Consequently, the explanation for the spatio-temporal variations in the index of inhibition must reside in the intrinsic properties of the different regions of the germinal epithelium. This implies that a progressive recovery of the attractive power, in a cranio-caudal direction, occurs in the presence of a constant concentration of inhibitor.

The previous measurements only provide an approximate notion of the extent of recovery of attractive forces, because they reflect overall values that include the resultant of earlier events. It is, however, possible to erase the "memory" component and consequently to obtain a more precise

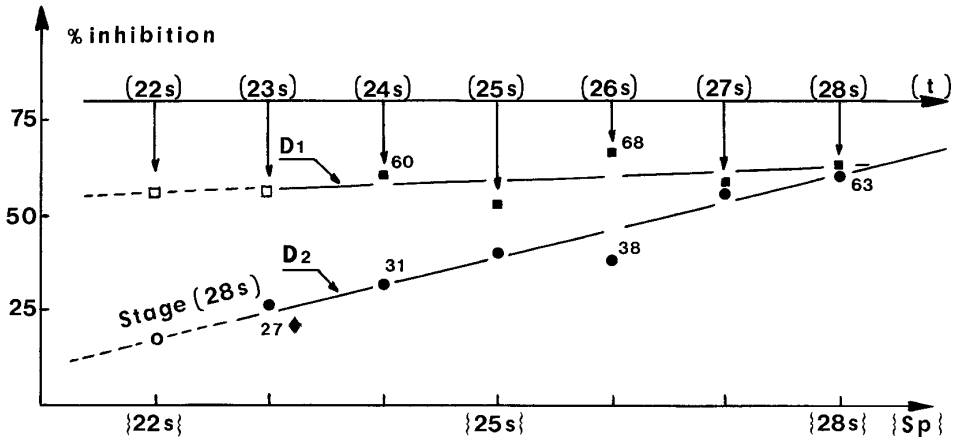

Figure 4. Variations in the level of inhibition (overall data) in space and time. ({s} regions for a DEXA concentration of 4.6×10^{-8} M; Tab. VI.) *Regression line* D_1: each triplet ({n_s}, (n_s), %) = (■) corresponds to the degree of inhibition in each of the {n_s} regions marked on the abscissa at the moment of the formation of the corresponding somite (n_s). Each of the 5 measurements was performed *successively* within the interval [(24s) to (28s)]. The degree of inhibition was constant (mean close to 60%). *Regression line* D_2: each triplet ({n_s}, (28s), %) = (●) corresponds to the degree of inhibition in each of the {s} regions in the space ({23s} – {28s}) at stage (28s). The 6 measurements were carried out *simultaneously*. The mean degree of inhibition was close to 40%.

description of the progression of events; this can be done by replacing the study of global phenomena by an analysis of the local and punctual increases ΔN_C and ΔN_D. Under these conditions, the coefficients of inhibition can be calculated from the formula: $(\Delta N_C - \Delta N_D) / \Delta N_C$ (Tabs. II and IV).

The calculations were carried out under diverse conditions that are detailed in Table VI, Section 2. Their examination clearly revealed that the intensity of inhibition declined regularly as a function of time in the most rostral regions, whereas the effect of DEXA remained stable in the most caudal regions of the gonadal primordium. At the end of the experimental period, the attractive power became completely re-established in the [{22s}→{24s}] regions. This total recovery explained why experimental embryos captured more PGC in this region than did control embryos (Tab. VI bis). The graphical representation of these facts is shown in Figure 5. In conclusion, the natural molecular forces underlying the attraction progressively overcome the effects of the experimentally applied inhibitor and restore the attractive field in its entirety. Furthermore, the mobility of the PGC was not affected by their continual exposure to the action of Dexamethasone throughout the experiment (Tab. VI bis).

3.2.5. Restoration of the attractive potential (AP) as a function of space and time (Fig. 6)

The ratio of the number (ΔN) of gonocytes captured per unit time to the number (N) of circulating PGC at the same instant defines the notion of "attractive potential" PA_C and PA_D for control and experimental embryos respectively. Observation and calculation concur to show that maximal inhibition occurred when and where the last somite was formed. Maximal inhibition was approximately 60% when the concentration

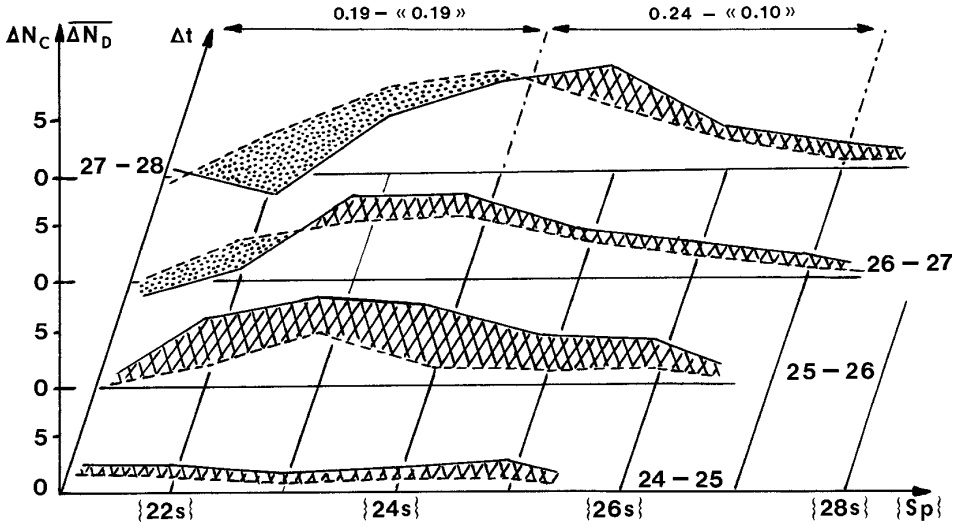

Figure 5. Evolution of local and punctual increases of N_C and $\overline{N_D}$ in space and time (mean concentration of DEXA: 4.6×10^{-8} M). Although the diagram displays a clear similarity with Figure 2, it differs fundamentally by virtue of the physical dimension of the process it represents. In the hatched areas the numbers of gonocytes captured per unit time in presence of the inhibitor are lower than those observed in controls: $(\Delta N_C - \Delta \overline{N_D}) > 0 \rightarrow$ inhibition. The situation is reversed in the dotted areas, where: $(\Delta N_C - \Delta \overline{N_D}) < 0 \rightarrow$ recovery of the attractive forces. One can calculate from these data the *real* degree of inhibition and the value of the potential of attraction in a given region of the gonadal primordium as a function of time (Tab. VI bis). The dotted area increases in the anterior {s} regions while the attractive field spreads in a caudal direction. In the anterior and posterior regions of the gonadal primordium we recall the coefficients of attraction measured, at the end of the experience, respectively in control embryos and in embryos cultivated in the presence of Dexamethasone (<< >>).

of DEXA was 4.6×10^{-8} M (see Fig. 4, line D_1). For the hypothetical competition between the natural promote of the attractive field and the inhibitor, the variation of the degree of restoration of the forces that underlie the chemotactism (measured by $\overline{PA_D}/PA_C$) can be represented on a scale graduated from 0.4 to 1, or from 0.3 to 1 when the DEXA concentration is increased to 1.8×10^{-7} M (level of inhibition ≅ 70%). Determination of $\overline{PA_D}/PA_C$ in the different {s} regions of the gonadal primordium at different stages of the experiment provides a description of the extent of recovery as a function of space and time. The results of the calculations applied to the data of Tables I to IV appear in Figure 6. The graphical representation clearly shows that a delay of approximately 4 hours elapsed before the first signs of the recuperation of the attractive forces became significantly apparent. This is why the attractive field at the end of the experiment (stage 28s) was completely (100%; see graph — ○ —, Fig. 6) or somewhat less than completely (≅ 80%; see graph ● — ●, Fig. 6) *restored* in the anterior regions, whereas the *level of inhibition* remained statistically stable (≅ 60% and ≅ 70%) in posterior regions, where differentiation occurred later (graphs – – Δ – – and ▲ – – – ▲).

Table VI bis. Potential of attraction in the anterior and posterior regions of the gonadal primordium – (stage 28s).

a./ Increases ΔN_C and $\overline{\Delta N_D}$ in the period Δt = [(27s) to (28s)]

DEXA Concentration	Stage (28s)			Stage (27s)			ΔN			$\Sigma \Delta N$
	{22}	{23}	{24}	{22}	{23}	{24}	{22}	{23}	{24}	{22-24}
0 (controls)	11.3	28.8	28.1	12.5	23.5	20	-1.2	5.3	8.1	12.2
$4.6.10^{-8}$ M	12.9	21	19.3	9.3	13.4	10.4	3.5	7.6	8.9	20
$1.8.10^{-7}$ M	11.6	18.4	16.5	7.8	11.8	9	3.8	6.6	7.5	18

b./ Coefficients of attraction in regions [{22s} → {24s}].

N.B. Under normal developmental conditions, approximately 170 PGC are involved in the fertilisation process. (see Figure 1).

At stage (27s)	Gonocytes captured	Transiting PGC	Coefficients
Controls	105	170-105 = 65	12.2/65 = 0.19
$4.6.10^{-8}$ M	(86.5+53+50)/3 = 63	170-63 = 107	20/107 = 0.19
$1.8.10^{-7}$ M	(86.5+53+50+31)/4 = 55	170-55 = 115	18/115 = 0.16

c./ Coefficients of attraction in regions [{25s} → {27s}].

Controls	105	65	15.5/65 = 0.24
$4.6.10^{-8}$ M	63	107	10.5/107 = 0.10
$1.8.10^{-7}$ M	55	115	8.5/115 = 0.07

Interpretation. The value of the coefficient of attraction ($\overline{\Delta N_D}$ gonocytes captured / $\overline{N_D}$ PGC in transit) corresponds to the intensity of attraction of the germinal epithelium in experimental embryos. There is inhibition when the coefficient is smaller than that of the controls (section c./). The recovery of the potential of attraction is complete when the coefficients are the same (section b./).

4. DISCUSSION

4.1. The attraction of the germinal epithelium

Our study demonstrates the existence of hitherto unknown properties of the gonadal primordium in Birds. The differentiation of the coelomic epithelium into an attractive germinal epithelium occurred both in space and time, in close correlation with somitogenesis in a region approximately limited by somites 22 to 30. The attractive forces were the most intense in regions [{23s}→ {25s}] and 75% of the population captured by stage (28s) were found in this zone.

Is the differentiation of the germinal epithelium under the control of the newly formed somites, as seems to be suggested by the strict synchrony between the occurrence of the two processes? Or is this coincidence due in fact to an intrinsic property, common to both systems, controlled by cell-autonomous processes linked to the general state of development of the embryo?

Work carried out on Anuran Amphibians [12, 13] has suggested that the interstitial migration that results in the displacement of the PGC from the ventral endoderm towards the dorsal mesentery is directed by dorsal mesodermal organs (notochord, somites and ureters). However, these conclusions can hardly be extrapolated to Birds, in which PGC transiting by the aortas and capillaries are directly exposed to the attraction of the GE.

The consequences of the imaginary subdivision of the gonadal primordium, by projection of the segmentation of axial structures, on the description and analysis of events occurring in this anatomically continuous rudiment are not indifferent. Is such a description, by successive steps, purely

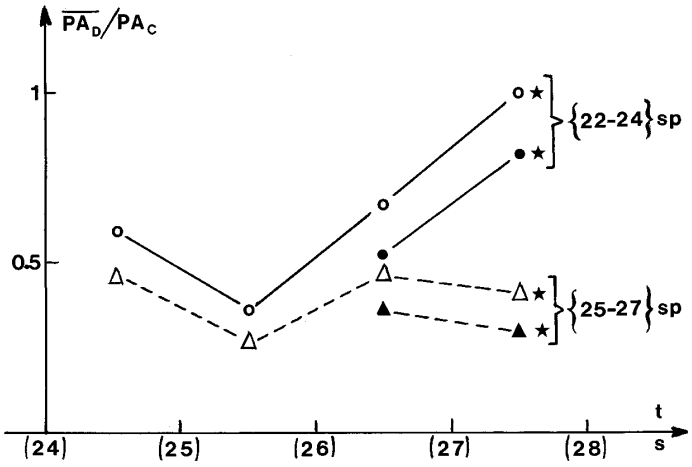

Figure 6. Graphical representation of the restoration of the attractive field in the presence of a constant concentration of dexamethasone. **(**1) *Restoration* in the anterior region {22s – 24s}: — ○ —, 4.6×10^{-8} M; ● — ●, 1.8×10^{-7} M DEXA. (2) The corresponding graphs (– – – △ – – – , and ▲ – – – ▲) show the stability of the level of *inhibition* of the attractive forces in the posterior region {25s – 28s} of the gonadal primordium. ★ For these values of the ratio $\overline{PA_D}/PA_C$ see Table VI bis, column "coefficients". See text for further explanation.

artificial or does it correspond to an underlying reality? In other words, is it justified to interpret the differentiation of the proximalmost part of the lateral plate in terms of a potentially metameric organisation? The antero-posterior progression of the differentiation of the attractive GE, rigidly coupled to the segmentation of the paraxial mesoderm, is a clearly demonstrated fact. The correspondence between the two events is such that it is possible to depict the spatiotemporal evolution of the fertilisation of the gonadal primordium by a description of the progression of somitogenesis. The heterogeneous distribution of the intensity of the power of attraction between the different virtual regions is also unquestionable. Furthermore, it should be noted that the ventrally situated GE, in a position far removed from the dorsal somites, captures the majority of its gonocytes from the source of PGC transiting via the splanchnopleural circulation. This eliminates the possibility of a direct influence of the segmented paraxial mesoderm on the coelomic epithelium.

In the light of these remarks, the hypothesis that the differentiation of the gonadal primordium is induced by intrinsic mechanisms genetically associated with the metameric organisation of the embryo is worthy of attention. The lateral plate is never morphologically segmented. However, the segmentation of the mesoderm that gives rise to the intermediate mesoderm is not constant. In Teleosts, it is even totally lacking in the trunk region, the only suspicion of its existence residing in its nephritic derivatives. Although this is an extreme example, it is nevertheless instructive in as much as it indicates that the molecular mechanisms controlling segmentation can be uncoupled from differentiation. Abortive segmentation clearly does not prevent the successful differentiation of the potentially metamerisable primordium: the metameric aspects of the differentiation of an organ

attest a posteriori to the imperceptible segmentation of the embryonic rudiment.

The initial stages of the ontogeny of the gonadal primordium in the chick displays indisputable similarities with other systems in which the activation of homeobox-containing genes have been implicated. However, to date no authors have reported the presence of homeotic gene transcripts in the PGC, the captured gonocytes or the germinal epithelia [3, 15, 19, 23, 30, 35, 36]. Further work is required in order to determine whether the most proximal region of the lateral plate expresses molecular vestiges of an ancestral metameric organisation.

4.2. Dexamethasone and inhibition of the fertilisation of the gonadal primordium

From a global phenomenological standpoint, the inhibition of the fertilisation of attractive GE may be due to a weakening either of the attractive forces or of the motility of the migratory PGC. These alternative explanations are not mutually exclusive and this leads to an ambiguity in the interpretation of the experimental results. In certain cases, the uncertainty can be removed with the aid of analytical treatment that enables a law of inhibition to be formulated. This applies, for example, to the effects of Concanavalin A: the form of the relationship (the log of the degree of inhibition increases proportionately to the concentration of lectin) points to the PGC as being the target of the inhibitor [9]. The theoretical implications of this law have recently been experimentally confirmed [4]. The action of DEXA, however, is completely different: in this case, and in agreement with the predictions of a well known rule of classical physiology, the coefficient of inhibition is proportional to the log of the concentration of glucocorticoid (Fig. 3). The explanation here is less certain and an earlier hypothesis attributes the diminished intensity of colonisation of the gonadal primordium to deficiencies in the proteolytic properties of the PGC [16]. According to this hypothesis, DEXA is proposed to act via complex mechanisms, involving the inhibition of macrophage migration, blocking the synthesis of the plasminogen activator [31]. However, despite subsequent efforts, no convincing evidence in favour of this explanation has been obtained (F. Chapeville, A.-L. Haenni, Z. Lassota, G. Desvages and R. Dubois, unpublished). More recent observations have shed some light on this lack of success: experimental exposure of a sexually undifferentiated gonad (6 days of incubation) to the attraction of a young GE (2.5 days of incubation) is known to reactivate the chemotactism of the primary gonocytes while simultaneously stimulating their synthesis of glycoprotein complexes [4]. Neither of these responses is observed in heterochronic associations cultured for six hours in the presence of DEXA (Dubois and Cuminge, unpublished observations). In the present study, we noted that the migratory properties of PGC exposed to DEXA in vitro for 12 hours or so remained unchanged (Tab. VI bis). It therefore seems that the chemotactism of different categories of cells (leukocytes, macrophages and PGC) does not have a common cause.

Since the motility of PGC was not altered by DEXA, the probable explanation of the perturbations triggered by the inhibitor is an alteration of the metabolism of the gonadal primordium.

The young gonade of avian embryo (5–6 days of incubation) possesses receptor sites for steroid [10], as well as key enzymes of steroid metabolism, notably aromatase [6] and $\Delta 5 - 3\beta -$ ol HSDH activities [34, 37]. Furthermore, the epithelial cells of the gonadal primordium are equipped to react with endogenous or exogenous steroid complexes: estrogen receptor (cER) transcripts have been detected in female tissues at day 3.5 of incubation (i.e., 3 days before morphological sexual differentiation) [29]. It is thus plausible that DEXA disturbs

steroid metabolism by interacting with cytosolic receptors. The strong functional homologies between steroid and corticoid receptors [1, 17] should be underlined in support of this hypothesis.

The current molecular model of steroid action involves associations between immunosuppressors (FK506, rapamycin, cyclosporin A), immunophilin ligands (FKBP59, cyclophilin 40) and heat-shock proteins (notably hsp 90) to form a complex that incorporates the hormone and its receptor [26]. These functional units are believed to play several important roles: stabilisation of the steroid-receptor interaction [2]; nuclear translocation of the hormone [5, 18, 24, 28]; and gene activation [11, 20, 27]. Thus, for example, the hypothesis of a thermally-induced modification, via hsp, has been invoked to explain the temperature-dependent sexual differentiation of certain Reptiles [25].

The crucial role of molecular chaperones in insuring the stability of the bonds between steroid and receptor may be of particular relevance to our results. It has been clearly demonstrated that the interaction between DEXA and steroid receptors is unstable and reversible [1]. Here we showed that a competition occurs between the inhibitor and the molecule (s) responsible for the process of germ cell attraction. A plausible site of action of a competitor is at the level of a receptor recognised both by DEXA and an endogenous activator. This hypothesis implies that the inhibitor does not block the synthesis of the natural promoter (in all probability a steroid-containing complex), which is ultimately able to displace the corticoid from the cytosolic receptor. Further research is required to determine whether and how steroids intervene at such an early stage in the sexual organogenesis of Birds.

The suggestion that the correct placing of the cells responsible for ensuring the continuity of the species is controlled by a highly conserved homeotic mechanism is not unreasonable. There is indeed evidence of analogies between the process of fertilisation of the gonadal primordium and the ontogeny of systems regulated by a Hox code. The role of homeogenes in the organisation of the embryo has been interpreted as a molecular explanation of the ancient theory of gradients: the attractive field that chemically guides the positioning of the germ cells in the gonadal primordium is nothing but a current version of the concept of a “morphogenetic field”, updated in terms of the expression of developmental genes.

ACKNOWLEDGMENTS

The authors wish to thank Drs J.M. Gasc and C. Pieau for valuable criticism of the manuscript and I. Dubois for secretarial assistance.

REFERENCES

[1] Baxter J.D., Tomkins G.M., Specific cytoplasmic glucocorticoid hormone receptors in hepatoma tissue culture cells, Proc. Nat. Acad. Sci. USA 68 (1971) 932–937.

[2] Cadepond F., Jibard Binart N., Schweizer-Groyer G., Segard-Maurel I., Baulieu E.E., Selective deletions in the 90 kDa heat shock protein impede hetero-oligomeric complex formation with the glucocorticosteroid receptor (GR) or hormone binding by GR, J. Steroid. Bioch. Mol. Biol. 48 (1994) 361–367.

[3] Coelho C., Sumoy L., Kosher R.A., Upholt W.B.G., Hox.7: a chicken homeobox-containing gene expressed in a fashion consistent with a role in patterning events during embryonic chick limb development, Differentiation 49 (1992) 85–92.

[4] Cuminge D., Dubois R., Données nouvelles sur le rôle des glycoprotéines dans le chimiotactisme des cellules germinales chez l’embryon de Poulet, C.R. Acad. Sci. Paris 320 (1997) 701–707.

[5] Czar M.J., Lyons R.H., Welsh M.J., Renoir J.M., Pratt W.B., Evidence that the FK 506-binding immunophilin heat shock protein 56 is required for trafficking of the glucocorticoid receptor from the cytoplasm to the nucleus, Mol. Endocrinol. 9 (1995) 1549–1560.

[6] Di Clemente N., Ghaffari S., Pepinsky R.B., Pieau C., Josso N., Cate R.L., Vigier B., A quantitative and interspecific test for biological activity of anti-Müllerian hormone: the fetal ovary aromatase assay, Development 114 (1992) 721–727.

[7] Dubois R., Cuminge D., La migration des cellules germinales chez l'embryon de poulet. I. Aspects cinétiques, Arch. Biol. (Bruxelles) 93 (1982) 185–242.

[8] Dubois R., Cuminge D., La migration des cellules germinales chez l'embryon de poulet. III. Aspects hémodynamiques et déterminisme de l'asymétrie de répartition des gonocytes, Arch. Biol. (Bruxelles) 93 (1982) 381–432.

[9] Dubois R., Cuminge D., La migration des cellules germinales chez l'embryon de poulet. IV. Interprétation des données quantitatives et cinétiques obtenues par l'emploi d'inhibiteurs de la motilité cellulaire, Arch. Biol. (Bruxelles) 95 (1984) 347–410.

[10] Gasc J.M., Stumpf W.E., Sexual differentiation of the urogenital tract in the chicken embryo: autoradiographic localization of sex-steroid target cells during development, J. Embryol. Exp. Morphol. 63 (1981) 207–223.

[11] Gasc J.M., Renoir J.M., Faber L.E., Delahaye F., Baulieu E.E., Nuclear localization of two steroid receptor-associated proteins, hsp 90 and p 59, Exp. Cell. Res. 186 (1990) 362–367.

[12] Giorgi P., Germ cell migration in toad (*Bufo bufo*): effect of ventral grafting of embryonic dorsal regions, J. Embryol. Exp. Morph. 31 (1974) 75–87.

[13] Gipouloux J.D., Recherches expérimentales sur l'origine, la migration des cellules germinales et l'édification des crêtes génitales chez les Amphibiens Anoures, Bull. Biol. Fr. Belg. 104 (1970) 21–93.

[14] Hamburger V., Hamilton H., A series of normal stages in the development of the chick embryo, J. Morphol. 88 (1951) 49–92.

[15] Izpisua-Belmonte J.C., Tickle C., Dolle P., Wolpert L., Duboule D., Expression of the homeobox Hox-4 genes and the specification of position in chick wing development, Nature 350 (1991) 585–589.

[16] Jakubowicz S., Effets de la Dexaméthasone sur la colonisation des ébauches gonadiques par les cellules germinales primordiales chez l'embryon de poulet, DEA, Université Paris VI, 1978.

[17] Jensen E.V., Suzuki T., Kawashima T., Stumpf W.E., Jungblut P.W., De Sombre E.R., A two-step mechanism for the interaction of estradiol with rat uterus, Proc. Nat. Acad. Sci. USA 59 (1968) 632–638.

[18] Jung-Testas I., Lebeau M.C., Catteli M.G., Baulieu E.E., Cyclosporin A promotes nuclear transfer of a cytoplasmic progesterone receptor mutant, C.R. Acad. Sci. Paris 318 (1995) 873–878.

[19] Kurutani S., Martin J.F., Wawersik S., Lilly B., Eichele G., Olson E.N., The expression pattern of the chick homeobox gene gMHox suggests a role in patterning of the limbs and face and in compartmentalization of somites, Dev. Biol. 161 (1994) 357–369.

[20] Lebeau M.C., Massol N., Herrick J., Faber L.E., Renoir J.M., Radanyi C., Baulieu E.E., P 59, an hsp 90-binding protein: cloning and sequencing of its c DNA and preparation of a peptide-directed polyclonal antibody, J. Biol. Chem. 267 (1991) 4281–4284.

[21] Lotka A.J., Elements of mathematical biology, Dover Publications, Inc., New York, 1956.

[22] Maynard Smith J., Mathematical Ideas in Biology, Cambridge University Press, Cambridge London New York Melbourne, 1968.

[23] Newman S.A., Sticky fingers: Hox genes and cell adhesion in vertebrate limb development, Bioessays 18 (1996) 171–174.

[24] Perrot-Applanat M., Cibert C., Geraud G., Renoir J.M., Baulieu E.E., The 59 kDa FK 506-binding protein, a 90 kDa heat shock protein binding immunophilin (FKBP59-HBI), is associated with the nucleus, the cytoskeleton and mitotic apparatus, J. Cell. Sci. 108 (1995) 2037–2051.

[25] Pieau C., Temperature variation and sex determination in reptiles, Bioessays 18 (1996) 19–26.

[26] Renoir J.M., Le Bihan S., Mercier-Bodard C., Gold A., Arjomandi M., Radanyi C., Baulieu E.E., Effects of immunosuppressants FK 506 and rapamycin on the hetero-oligomeric form of the progesterone receptor, J. Steroid. Bioch. Mol. Biol. 48 (1994) 101–110.

[27] Renoir J.M., Mercier-Bodard C., Hoffmann K., Le Bihan S., Ning Y.M., Sanchez E.R., Hand-Schumacher R.E., Baulieu E.E., Cyclosporin A potentiates the dexamethasone-induced mouse mammary tumor virus. Chloramphenicol acetyltransferase activity in LMCAT cells: A possible role for different heat shock protein-binding immunophilins in glucocorticosteroid receptor-mediated gene expression, Proc. Nat. Acad. Sci. USA 92 (1995) 4977–4981.

[28] Sabbah M., Radanyi C., Redeuilh G., Baulieu E.E., The 90 kDa heat-shock protein (hsp 90) modulates the binding of the oestrogen receptor to its cognate DNA, Biochem. J. 314 (1996) 205–213.

[29] Smith C.A., Andrews J.E., Sinclair A.H., Gonadal sex differentiation in chicken embryos: expression of estrogen receptor and aromatase genes, J. Steroid. Biochem. Mol. Biol. 60 (1997) 295–302.

[30] TakahashiY., Bontoux M., Le Douarin N.M., Epithelio-mesenchymal interactions are critical for Quox 7 expression and membrane bone differentiation in the neural crest derived mandibular mesenchyme, EMBO J. 10 (1991) 2387–2393.

[31] Vassali J.D., Hamilton J., Reich E., Macrophage plasminogen activator: modulation of enzyme production by anti-inflammatory steroids, mitotic inhibitors and cyclic nucleotids, Cell 8 (1976) 271–281.

[32] Wolff E., Haffen K., Sur une méthode de culture d'organes embryonnaires in vitro, Texas Report Biol. Med. 10 (1952) 463–472.

[33] Wolff E., Simon D., L'explantation et la parabiose in vitro de blastodermes incubés d'embryons de Poulet. L'organisation de la circulation extraembryonnaire, C.R. Acad. Sci. Paris 241 (1955) 1994–1996.

[34] Woods J.E., Erton L.H., The synthesis of estrogens in the gonads of the chick embryo, Gen. Comp. Endocrinol. 36 (1978) 360–370.

[35] Xue Z.G., Gehring W.J., Le Douarin N.M., Quox-1 a quail homeobox gene expressed in the embryonic central nervous system, including the forebrain, Proc. Natl. Acad. Sci. USA 88 (1991) 2427–2431.

[36] Xue Z.G., Xue X.J., Le Douarin N.M., Quox-1 an Antp like homeobox gene of the avian embryo: a developmental study using a Quox-1 specific antiserum, Mech. Dev. 43 (1993) 149–158.

[37] Yoshida K., Shimada K., Saito N., Expression or P 450 17α-hydroxylase and P 450 aromatase genes in the chicken gonad before and after sexual differentiation, Gen. Comp. Endocrinol. 102 (1996) 233–240.